Size calibration of strained epitaxial islands due to dipole-monopole interaction

V. I. Tokar and H. Dreyssé

IPCMS, Université de Strasbourg–CNRS, UMR 7504, 23 rue du Loess, F-67034 Strasbourg, France

E-mail: tokar@unistra.fr

E-mail: hugues.dreysse@unistra.fr

Abstract. Irreversible growth of strained epitaxial nanoislands has been studied with the use of the kinetic Monte Carlo (KMC) technique. It has been shown that the strain-inducing size misfit between the substrate and the overlayer produces long range dipole-monopole (d-m) interaction between the mobile adatoms and the islands. To simplify the account of the long range interactions in the KMC simulations, use has been made of a modified square island model. Analytic formula for the interaction between the point surface monopole and the dipole forces has been derived and used to obtain a simple expression for the interaction between the mobile adatom and the rectangular island. The d-m interaction was found to be longer ranged than the conventional dipole-dipole potential. The narrowing of the island size distributions (ISDs) observed in the simulations was shown to be a consequence of a weaker repulsion of adatoms from small islands than from large ones which led to the preferential growth of the former. Furthermore, similarly to the unstrained case, the power-law behavior of the average island size and of the island density on the coverage has been found. In contrast to the unstrained case, the value of the scaling exponent was not universal but strongly dependent on the strength of the long range interactions. Qualitative agreement of the simulation results with some previously unexplained behaviors of experimental ISDs in the growth of semiconductor quantum dots was observed.

Keywords: irreversible aggregation phenomena (theory), thin film deposition (theory), heteroepitaxy (theory) molecular beam epitaxy (theory)

1. Introduction

The phenomenon of self-assembly of size-calibrated coherent nanoislands taking place in some heteroepitaxial systems during strained epitaxy has been extensively studied for more than two decades because of its prospective use in microelectronics [1, 2]. It seems to be well established that the phenomenon is governed by the elastic strain in the overlayer caused by the lattice size misfit with the substrate [1, 2]. Usually, it is assumed that the main role in the size calibration (SC) play the long range forces propagated via the elastic strain in the substrate [3, 4, 5]. However, explicit growth simulations with the use of the kinetic Monte Carlo (KMC) technique within the models accounting for such forces in [6, 7, 8], did not show any narrowing of the island size distributions (ISDs). Moreover, in [6] even some broadening of the ISD was seen. Notably, the broad ISDs obtained in the simulations were very similar to those seen during irreversible growth [9]. So by all evidence the growth in [6, 7, 8] was controlled by kinetics; this is farther supported by the fact that in thermodynamically controlled strained epitaxy in [10, 11] ISDs narrowing were observed. These results seems to suggest that the SC is implausible under conditions of kinetically controlled growth. Such growth, however, usually takes place at smaller temperatures and at faster deposition rates than the thermodynamically limited growth [10] which presents some important practical advantages. For example, smaller substrate-deposit interdiffusion and so better control in heteroepitaxial growth [12]. Therefore, the question of whether the SC may be achieved under conditions of kinetically controlled growth is of considerable practical interest.

The aim of the present paper is to suggest a new mechanism of the SC during irreversible growth underlain by the repulsive long-range forces induced by the misfit strain. In contrast to the thermodynamically controlled growth when the conventional dipole-dipole (d-d) interatomic interactions [3, 4] are sufficient to ensure the SC [10], the d-d forces are too weak to assure SC in the kinetically controlled case, as the explicit simulations in [6, 7, 8] and our arguments in section 3 below show. However, it is known that besides the dipole forces at the strained surfaces there also exist monopole forces that are of longer range than the d-d interactions and in the case of the step-bounded surface structures, such as steps, islands, and pits play a dominant role in their energetics and kinetics [5, 13, 14, 15, 16, 17, 18].

In the present paper we will show that the monopole forces interacting with the force dipoles induced by the mobile adatoms play similarly important role in the growth kinetics. In particular, they provide a mechanism of the SC during irreversible growth. As will be shown in section 3, in the presence of d-m interactions the strength of the repulsion between the island and the mobile atom may grow with the island size in such a way that the atoms will avoid larger islands by preferentially attaching to smaller ones, thus making the island sizes more homogeneous. The explicit confirmation of this mechanism in explicit KMC simulations will be provided in section 4. But because the main difficulty in studying the strained epitaxy with the KMC technique is the necessity of accounting for the long-range interactions acting between all atoms in the

simulated system, essential simplifications and approximations are necessary to make the simulations feasible. The approximations used in KMC simulations in [10, 6, 7, 8] with the d-d interactions are not suitable for the d-m case. Therefore, in sections 2 we will introduce a simple model of strained islands, in section 3 will calculate the strain-induced interactions between the adatoms and the islands in the planar approximation, and in section 4 will explain the approximate description of the capture of the mobile adatoms by the square islands. Also, in this section we discuss the applicability of our results to the explanation of experimental data on the SC of the quantum dots in Ge/Si(001) system studied in [19, 20].

In the final section we present our conclusions.

2. The model of strained islands

The main problem in KMC simulation of many-body systems with long-range interactions is that to simulate the change of the position of a single atom, the energy of its interaction with all other atoms in the system need be calculated first. And in the case of the Metropolis algorithm [21] which is quite appropriate in this case (at sufficiently high temperatures, at least), the calculation need to be performed twice: for the initial and the final positions of the moving atom. And in the end the move can be discarded by the algorithm.

Because one is usually interested in the thermodynamic limit, the simulated system should be reasonably large to mitigate the finite-size effects. For example, in our simulations we used, following [10], the system consisting of 250×250 sites on a square substrate lattice. With maximum coverage $\theta = 0.2$ chosen to remain in precoalescence growth regime [9] our system contained up to 12500 atoms. In order to be able to calculate the interaction with all of them at each KMC step we had to simplify the task by adopting several simplifying assumptions. In particular, we assumed that due to the fast intraisland diffusion the islands acquire simple quasiequilibrium symmetric shapes that can be found with the use of the Wulff construction [22]. This approach has been widely used in simulations of unstrained epitaxial growth [23, 24, 6, 25, 26, 27] so below we adopt it to our needs. In particular, this will allow us to make comparison of our results with experiments on the growth of three-dimensional quantum dots (QDs) because crucial to our SC mechanism will be only the island-substrate interface and the shear strain propagated by it. So though in our simulations we use monolayer-high islands, if the base layer of a QD is size calibrated, the height (hence, the volume) that can be found via the Wulff construction will be also subject to the SC [22]. In the present paper, however, we will restrict our simulations to the simplest case of monolayer-high (or submonolayer [28]) islands.

Submonolayer islands on the square substrate lattice at low temperature will strive to acquire rectangular shapes [29]. In the harmonic approximation the elastic forces in orthogonal directions decouple. This allows one to treat the elastic relaxation independently within each linear atomic chain that compose the island [30, 11]. Another

simplification is to neglect the displacements of the surface atoms in the direction perpendicular to the surface, as suggested in [3, 4, 31]. This leaves us with one-dimensional (1D) chains of atoms lying at the rigid substrate [30, 11]. Their relaxation can be described within the harmonic Frenkel-Kontorova model as follows [30]. In this model the atoms are harmonically bound to the substrate sites, so the point monopole forces applied to the deposition cites in the in-plane directions are proportional to the atomic displacements and the stiffness k.

The displacements u_j of atoms $j = 1, 2, \ldots, l$ within a chain consisting of l atoms can be calculated as

$$u_j = f \sinh[\phi(2j - l - 1)]/[\sqrt{\alpha} \cosh(\phi l)], \tag{1}$$

where f is the size misfit between the substrate and the overlayer, $\alpha = k/k_{NN}$ the ratio of the rigidities of the elastic springs binding the atom to the substrate k and to the nearest neighbor atom k_{NN} and

$$\phi = \ln(\sqrt{1 + \alpha/4} + \sqrt{\alpha}/2). \tag{2}$$

In (1) and everywhere below all lengths are measured in the substrate lattice units (l.u.). So that the numerical value of the misfit parameter f coincides with the relative misfit. In Ge/Si(001), for example, $f = 0.042$ because the relative misfit in the system is 4.2%. We used this value of f together with small value of α in figure 1 to schematically illustrate the distribution of the atomic displacements inside atomic chains of different length.

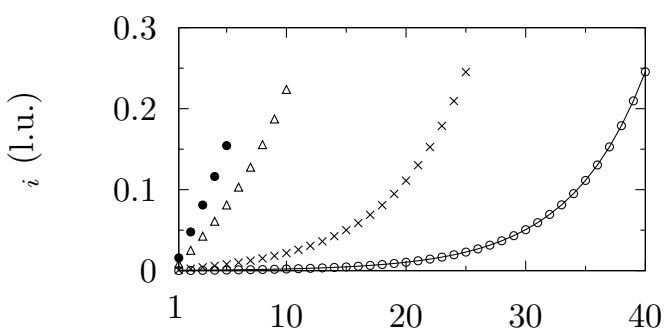

Figure 1. Symbols: Atomic displacements calculated according to (1) with $\alpha = 0.025$ and $f = 0.042$ for the chains consisting of (from left to right) 10, 20, 50 and 80 atoms. Only one half of the displacements are shown; the other half has the same values but the opposite sign. The solid line shows the displacements of the end 40 atoms of an infinitely long chain.

The small value of α in the figure was chosen to be close to the rigid-core case corresponding to $k_{NN} \to \infty$ and $\alpha \to 0$. As can be seen from (1) and (2), in this case

$$u_j = f(2j - l - 1)/2, \tag{3}$$

i. e., the atomic displacements depend linearly on the distance from the middle of the chain [11]. As we will show in the next section, the SC may take place in islands

where the atomic displacements and as a consequence the monopole forces grow with the island size. It is this type of islands that we will use in our KMC simulations in section 4. But obviously that in reality the atoms are not absolutely rigid and the compressibility ($1/k_{NN}$) is finite, though it can be small. From figure 1 it is seen that the displacements follow the linear behavior (3) only in sufficiently small islands. In large islands the displacements and the monopole forces saturate and phenomenologically can be described by constant monopole force density at the island edge, as in [5, 13, 14, 15, 16, 17, 18]. In this case the small and large islands repulse mobile monomers with similar force so our SC mechanism became inefficient.

The discrete strain can be calculated as (assuming the chain is oriented in the x direction)

$$\varepsilon_{xx} = \Delta u/\Delta x = u_{i+1} - u_i \tag{4}$$

because the x-coordinate difference is equal to 1 l.u.. As can be seen from figure 1, the average strain in small islands has appreciable value which diminishes with growing island size. In large islands strain remains only in the ends of the chain, so the average strain will tend to zero as $1/l$. It is exactly the behavior found in square Co islands on the Cu(001) surface in *ab initio* molecular dynamics simulations in [32]. The authors assess that the saturation starts in islands of ~ 2 nm size. Size-calibrated metallic islands of similar sizes are needed to produce efficient catalysts [33], so our SC mechanism can be of practical importance in this field.

3. Long range elastic interactions on the surface

In this section we derive expressions for the substrate-propagated elastic interactions to be used in KMC simulations in section 4. Due to the long-range nature of the interactions [34], the hopping adatom interacts with all other atoms on the surface. In order to calculate the interaction with the large number of atoms at each atomic hop, computationally efficient expressions for the interaction energy are needed.

As was explained previously, such expressions can be derived for epitaxial islands of simple geometry. Thus, following [23, 24, 6, 25, 26, 27] we assume that at low temperature the islands on the square substrate lattice acquire rectangular shapes and will derive the expressions for the interaction of the mobile monomers with such islands.

3.1. The dipole-dipole interaction

First we show that the conventional dipole forces are not sufficiently strong for the above SC mechanism to be operative. The potential acting between two adatoms at distance r apart in this case is [3, 4]

$$V^{\mathrm{d-d}} = \frac{\gamma}{r^3}, \tag{5}$$

where $\gamma > 0$ is the interaction strength and r , so r is dimensionless and the closest atoms are 1 l.u. apart.

Now assuming the atoms form a rectangle with sides a and b along the x and y directions, respectively, and summing contributions of the form of (5) over all atoms within the island in the continuum approximation one gets:

$$V_{ab}^{\mathrm{d-d}}(x,y) = \gamma\Big[\Big[\frac{\bar{r}}{\bar{x}\bar{y}}\Big]_{\bar{x}_-}^{\bar{x}_+}\Big]_{\bar{y}_-}^{\bar{y}_+}. \tag{6}$$

Here two-dimensional radius vector $\mathbf{r} = (x, y)$ points from the island center which we placed for simplicity at the coordinate origin $(0, 0)$ to the position of the mobile atom; $\bar{x}_\pm = x \pm a/2$, $\bar{y}_\pm = x \pm b/2$, and $\bar{r} = (\bar{x}^2 + \bar{y}^2)^{1/2}$. The square brackets in (6) denote the substitution of four possible combinations of $\bar{x}_\pm, \bar{y}_\pm$ for $\bar{x}$ and $\bar{y}$ with necessary signs.

Rectangular islands were grown in the KMC simulations in [6] but no narrowing of the ISDs was found. Equation (6) allows us to understand this. According to [35] the island capture numbers in the rate equations that define the rate at which the islands capture the mobile adatoms is proportional to the density of the adatoms at the sites situated one hopping step away from the island. They may be called the island nearest neighbors (NN). At high values of the diffusion to deposition rates ratio that we are going to simulate in section 4 the growth is in the thermodynamically controlled regime the distribution of mobile atoms is very close to equilibrium [10, 11] so their density can be assessed as

$$N_{1NN} \propto \exp[-E(i_{NN})/k_B T], \tag{7}$$

where $E(i_{NN})$ is the energy of the adatom at some point i_{NN} NN to the island. Let us for definiteness consider the point $i_{NN} = (a/2 + 1, 0)$, at 1 l.u. distance from the middle of the edge of length a of an island centered at the coordinate origin $(0, 0)$. From (6) it is easy to see that at large a, b $E(i_{NN}) = V_{ab}^{\mathrm{d-d}}(a/2 + 1, 0)$ saturates to a constant value. Thus, the mobile atoms can reach both large and small islands with equal ease, so the d-d repulsion does not cause SC during irreversible growth.

3.2. The monopole-dipole interaction

The dipole-dipole interactions correspond to the situation when each adatom is positioned in the geometric center of the substrate lattice unit cell so all atomic displacements in the substrate are also symmetric and the resulting force distribution corresponds to the force dipole. Such a behavior would describe rather non-strained situation because the presence of a positive misfit f means that the adatoms are too big to fit into the substrate cells without pushing their neighbors. This situation can be described within the model of the rigid-core adatoms [11] which should be adequate for situations where $f > 0$ and the atomic relaxation in the island base layer is small. Thus, it is easy to see from (3) that if the diameter of the rigid core is $1 + f$, then the atom with the coordinates $\mathbf{r} = (x, y)$ inside the island centered at the origin will be displaced by its neighbors from the center of the lattice cell it belongs to in the direction $\mathbf{r}$ as

$$\Delta\mathbf{r} = f\mathbf{r}. \tag{8}$$

[11]. But the adatoms are bound to the substrate cell centers by an effective harmonic spring with the spring constant k. So the displaced adatom at position $\mathbf{r}$ within the island will exert on the substrate a shear force in the $x-y$ plane with the density

$$\mathbf{F}^m(\mathbf{r}') = k\Delta\mathbf{r}\delta(\mathbf{r}-\mathbf{r}') = kf\mathbf{r}\delta(\mathbf{r}-\mathbf{r}'), \tag{9}$$

where for simplicity we again resorted to the continuum approximation. We supplied the force density with the superscript "m" to stress its monopole character. Of course, there always exists an atom at $\mathbf{r}=-\mathbf{r}$ with the opposite force density so that at large distances from the island the potential will have the dipole-dipole asymptotic of the type of (5). In large islands, however, the distance $2r$ between the atoms can be large so an adatom approaching the island boundary will experience effectively the monopole forces.

The energy of interaction of an adatom with a force monopole is the work performed by the dipole force distribution $\mathbf{F}^d$ along the field of displacements $\mathbf{u}$:

$$V^{\mathrm{d-m}}(\mathbf{r}) = -\int \mathbf{F}^d(\mathbf{r}-\mathbf{r}')\cdot\mathbf{u}(\mathbf{r}')\,dx'dy'. \tag{10}$$

The dipole force distribution produced by an adatom at $\mathbf{r}$ is [4]

$$\mathbf{F}^d(\mathbf{r}-\mathbf{r}') = A\nabla\delta(\mathbf{r}-\mathbf{r}'), \tag{11}$$

where A is a constant. The displacement field due to the monopole force $\mathbf{F}$ applied at the coordinate origin for the isotropic case was calculated in [34]. So substituting expressions (8.19) for $\mathbf{u}(\mathbf{r})$ from that reference together with (11) into (10) one finds after some algebra

$$V^{\mathrm{d-m}}(\mathbf{r}) = \frac{A(1-\nu)}{2\pi\mu}\frac{\mathbf{F}\cdot\mathbf{r}}{r^3}, \tag{12}$$

where ν is the Poisson ratio and μ the shear modulus. As is seen, the interaction in (12) is longer-ranged than in (5). We remind that everywhere in the present study we, following [3, 4], consider only 2D in-plane forces and other vectors, so the component of the monopole force in the direction perpendicular to the surface was set to zero in expressions (8.19) from [34]. In more sophisticated models of strain in epitaxial islands (see, e. g., [36]) this component is non-vanishing and should be included in (12) along the line of derivation presented above.

Now substituting (9) into (12) and integrating over the rectangular island $a\times b$ centered at the origin $(0,0)$ one gets the potential of interaction with the adatom placed at the point (x,y) external to the island as

$$V_{ab}^{\mathrm{d-m}}(x,y) = C\Big[\Big[(x+\bar{x})\ln(\bar{y}+\bar{r}) + (y+\bar{y})\ln(\bar{x}+\bar{r})\Big]_{\bar{x}_-}^{\bar{x}_+}\Big]_{\bar{y}_-}^{\bar{y}_+}, \tag{13}$$

where $C = Akf(1-\nu)/2\pi\mu$ and other notation is the same as in (6).

To farther simplify the simulations, below we will assume that the islands are of square shape [23, 24, 25] because in the case of weak elastic forces and small islands we are going to study the aspect ratios of the rectangular islands are known to be close to unity [6, 18].

The potential (13) on the nearest-neighbor distance from the square island boundary

$$E(i_{NN}) = V_{aa}^{\mathrm{d-m}}(a/2+1,0)|_{a\to\infty} \sim Ca\ln a \tag{14}$$

which means that in contrast to the potential (6) derived from the dipole-dipole interaction, the potential based on the dipole-monopole forces does differentiate between mobile adatom capture by large and small islands, as can be seen from (7),—thus providing a mechanism for kinetically controlled SC.

4. KMC simulations of the growth of the square islands

To assess the efficiency of the proposed mechanism, kinetic Monte Carlo (KMC) simulations were carried out with the use of a variant of the square-island model developed in [23, 24, 25]. As explained in the previous section, to simplify the calculation of the elastic forces we slightly modified the model by applying the approach of [26, 27] to the square islands instead of the circular ones. Namely, we assumed that the side length of the island $a = \sqrt{s}$, where s is the island size. Then the square capture zone [9] with the side length $a + 2$ is formed by surrounding the island with a strip of width 1. Any atom that enters the capture zone either by direct impingement or via the hopping diffusion is irreversibly caught by the island whose size becomes $s + 1$.

4.1. Growth in the absence of elastic interactions

To validate our KMC setup we first carried out the simulations without the long-range interactions. Two points could arose concern in connection with our approach. First, because the capture of the monomers by the islands is different from the conventional square island model [23, 24, 25], the question arises on whether the physics of the growth remains qualitatively the same. Second, because of the difficulties with accounting for the interaction of the diffusing monomer with all atoms in the system, the size of the simulated lattice was chosen to be 250×250 sites which is smaller than typically used for the simulations of the growth without long-range interactions. Because our main interest in the present study are the ISDs, we compared the total number of atoms in two-dimensional square islands obtained in our approach with corresponding results from [6, 25]. The diffusion constant was calculated according to the standard expression

$$D = \nu_{\mathrm{att}} \exp(-E_d/k_B T)$$

with typical values for the attempt frequency $\nu_{\mathrm{att}} = 1$ THz, the diffusion barrier $E_d = 0.7$ eV [11], and the deposition rate 1.4 ML/min [19]. To gather good statistics simulations were repeated from 160 to 480 times so that the statistical errors in our data are very small usually not exceeding the sizes of the symbols used to plot the data.

We first checked the soundness of our approximations by simulating the growth without elastic forces and comparing the results with simulations on similar models of

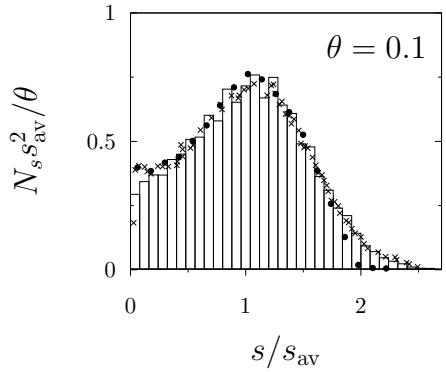

Figure 2. Simulated ISD for irreversible growth at 400 °C in the absence of misfit strain in our model (histogram); for comparison are shown simulation data from [6] (filled circles) and [25] (crosses)

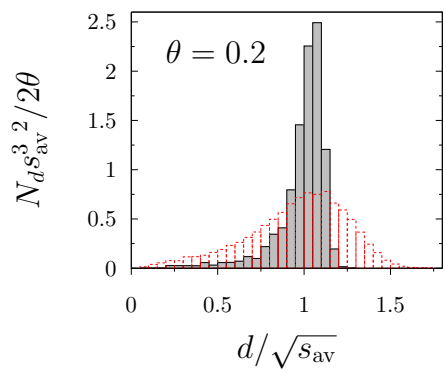

Figure 3. Shaded histogram—distribution of the diameters (defined as $d = \sqrt{s}$) of the islands grown in the KMC simulations at 400 °C with the elastic interaction corresponding to $\gamma = 20$ meV. The dashed histogram is the diameter distribution for $\gamma = 0$.

compact islands. The data shown in figure 2 are plotted in the scaling variables [9], as is conventional in the precoalescence regime at coverage θ not exceeding ~ 0.2:

$$N_s = \theta f(s/s_{\rm av})/s_{\rm av}^2, \tag{15}$$

where N_s is the density of islands of size s, $s_{\rm av}$ is the average island size, and f a universal scaling function. As is seen, the agreement is very good; most importantly, no ISD narrowing is seen in our data which means that the SC obtained in the simulations shown on figure 3 is due to the strain and not because of the approximations made.

4.2. KMC simulation of strained epitaxy

To simulate the growth with realistic strain in our model we need to chose the value of the constant C in (13). For consistency we chose it in such a way that islands with $a = 1$ corresponding to isolated adatoms asymptotically reproduced the dipole-dipole potential (5). After some algebra the asymptotic of (13) was found to be $C/(12r^3)$,

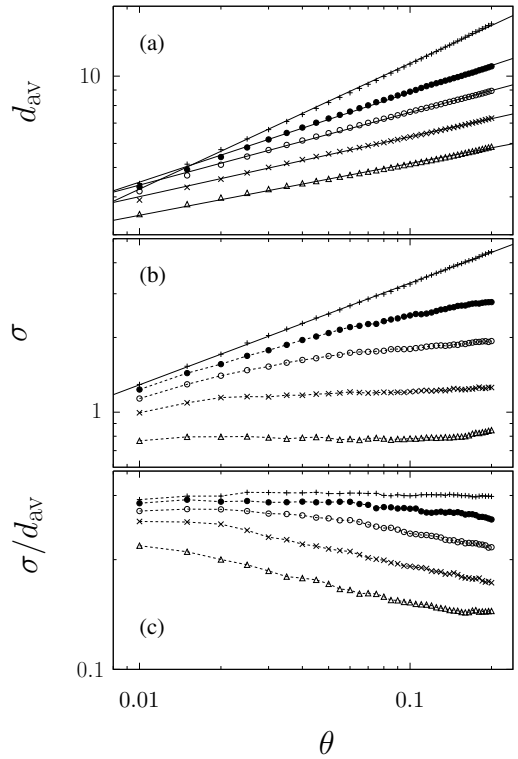

Figure 4. Log–log plots of the coverage dependences of the mean islands diameters (a), of the diameter distributions dispersions (b), and of the dispersion to the diameter ratios (c) for five values of the interaction parameter γ: 0 (+), 2.5 meV (•), 5 meV (∘), 10 meV (×), and 20 meV (Δ). Solid lines are linear fit to the data; dashed lines are guides to the eye. Note that only $\gamma = 0$ data exhibit the scaling behavior.

so $C = 12\gamma$ would assure that at distances larger than 1 l.u. the interaction of an island consisting and of an adatom will have the same strength as the adatom-adatom interaction (5).

The range of numerical values of γ used in the simulations was chosen according to estimates made in [7, 6, 3]. Because the estimated values vary in a rather broad range and *ab initio* estimates of non-local interactions are known to be unreliable [37], the simulations were carried out for five values of $\gamma = 0$, 2.5, 5, 10 and 20 meV.

The main results of our KMC simulations are shown in figures 4 and 5 Two conclusions can be drawn from the data. The value of index ω introduced in [38] from the power-law dependence

$$s_{\rm av} \propto \theta^{-\omega} \tag{16}$$

can be found from our data on $d_{\rm av} \simeq \sqrt{s_{\rm av}} \propto \theta^{-\omega/2}$. This index is convenient for experimental measurement because it is directly connected to the index characterizing the total island density

$$N = \theta/s_{\rm av} \propto \theta^{1+\omega} \tag{17}$$

Our first conclusion is that the index strongly depends on the strength of the elastic

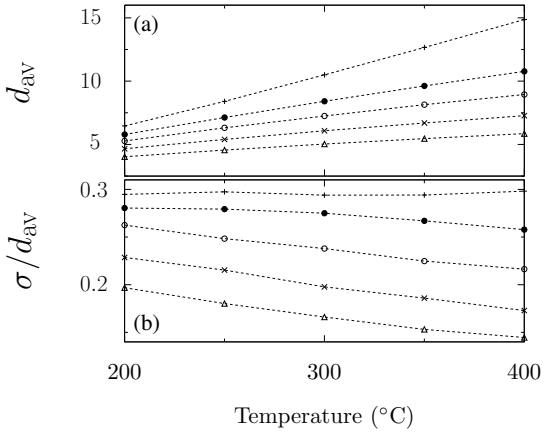

Figure 5. Temperature dependences of the mean island diameter $d_{\rm av}$ (a) and of the ratio of the diameter distribution dispersion σ to $d_{\rm av}$ (b) at coverage $\theta = 0.2$ for different strength of the elastic interaction; notation is the same as in figure 4.

γ(meV)	ω
0	-0.82
2.5	-0.59
5.0	-0.48
10.	-0.39
20.	-0.34

Table 1. Dependence of the scaling exponent ω as defined in (16-17) on the strength of the long-range interaction parameter γ (5)

forces, especially at small γ, as can be seen from table 1. Experimentally the smaller values of ω may look as the growth saturation, as seems to be the case in [39]. The second conclusion is that in the presence of strain the dispersion σ of the island diameter distribution (IDD) exhibits a saturated behavior, as can be seen from figure 4(b). In combination with monotonous growth of $d_{\rm av}$ the dispersion to mean diameter ratio diminishes with coverage in qualitative agreement with experimental data [39].

4.3. Discussion

The dispersion to mean diameter ratios in figures 4(c) and 5(b) are not as small as in some experimental data that exhibit the best cases of SC. One of reasons is that in our calculations we used the standard formulas of statistics and took into account all available IDD data from the smallest to the largest island sizes. Because they contain a tail in the IDD curves at small diameters (see figure 3), the values of $d_{\rm av}$ are smaller than diameter values at the IDD maxima. This augments both σ and $\sigma/d_{\rm av}$ values. Here it is pertinent to note that similarly asymmetric IDDs are rather commonly observed experimentally (see, e. g., [39, 20, 19, 40]). But because experimental data as a rule contain more different structures than exists in our simple model, size distributions for

islands of different morphologies are usually studied separately. Therefore, usually only the data in the vicinity of the maximum density of islands of a given morphology are taken into account in the processing of experimental data. Thus, for example, the value of the diameter at the IDD maximum for a given kind of islands is taken for $d_{\rm av}$ and the IDDs widths are calculated only in its vicinity [39, 20, 19]. In [39], for example, the relative FWHM with respect to $d_{\rm av}$ taken to be equal to d at the IDD maximum was found to be quite small (15%). But as can be seen from our figure 3, in our case it has similar value $\sim 14\%$. It is also common to fit experimental IDD with the Gaussian curve. But for the latter the WFHM$\approx 2.35\sigma$ so the effective value of $(\sigma/d_{\rm av})_{eff}$ with such data processing can be as small as 0.06. Thus, the SC mechanism proposed may underly even the best cases of SC seen experimentally.

5. Conclusion

To conclude, in this paper we suggested a kinetic mechanism of the SC in strained epitaxy. It differs from the kinetic mechanisms in the presence of the Ostwald ripening [39, 40] in that there is no need for atomic detachments. This means that the mechanism can be operative at smaller temperatures which may have important practical advantages. But because of similar growth behavior, the mechanism can also contribute to the phenomena attributed to the ripening. Furthermore, it may underly the unusual narrowing of IDD with temperature observed in the QDs growth in [20, 19] (cf. our figure 5). Such behavior is qualitatively different from that observed both in thermodynamically controlled growth and in the kinetically controlled growth in the absence of strain.

The proposed mechanism of SC heavily relies on the island size dependent monopole forces due to the misfit shear strain in the substrate, so the strength and spatial extent of the forces are of crucial importance. The simple rigid-core model [11] we used to illustrate our mechanism is presumably good for small islands simulated in the present paper and for those grown experimentally in [12]. For very large islands, however, saturation toward the constant monopole density similar to that on the surface steps should be expected. Calculations in [41] revealed the shear strain that linearly varies across the QD/substrate interface in capped InAs/GaAs pyramids of at least 12 nm in diameter. Experimentally large interface shear strain of considerable spatial extent caused by Ge/Si(001) QDs of an order of magnitude larger diameter was observed in [42]. This may mean that the mechanism described in the present paper contributes to the SC of QDs of all sizes. But even restricted to islands a few nanometer in diameter, the mechanism would still be of considerable practical interest. The maximal catalytic efficiency is achieved in size calibrated metallic islands of small diameters [33]. In semiconductor heteroepitaxy the quantum size effect that allows for variation of the QD photoluminescence wavelength is operative only in small QDs. Finally, the model of monolayer-high islands that we studied in the present paper can be taken as a starting point for modeling the growth of the submonolayer QDs [28]. Their small

spatial dimensions may allow for the fabrication of the most compact QD devices due to dense QD packing.

Finally, in the course of our study we derived a simple expression for the dipole-monopole interaction for in-plane displacements and forces that can be generalized to 3D in case of necessity. This expression can be used in other studies of nucleation and growth unrelated to SC. For example, in studying the influence on the growth of the surface steps, islands and pits that are usually present in strained epilayers.

References

[1] Stangl J, Holý V and Bauer G, *Structural properties of self-organized semiconductor nanostructures*, 2004 *Rev. Mod. Phys.* **76** 725

[2] Aqua J-N, Berbezier I, Favre L, Frisch T and Ronda A, *Growth and self-organization of SiGe nanostructures*, 2013 *Phys. Reports* **522** 59

[3] Lau K H and Kohn W, *Elastic interaction of two atoms adsorbed on a solid surface*, 1977 *Surf. Sci.* **65** 607

[4] Marchenko V I and Parshin A Y, *Elastic properties of crystal surfaces*, 1980 *Sov. Phys. JETP* **52** 129

[5] Tersoff J and Tromp R M, *Shape transition in growth of strained islands: Spontaneous formation of quantum wires*, 1993 *Phys. Rev. Lett.* **70** 2782

[6] Nandipati G and Amar J G, *Effect of strain on island morphology and size distribution in irreversible submonolayer growth*, 2006 *Phys. Rev.* B **73** 045409

[7] Aqua J-N and Frisch T, *Elastic interactions and kinetics during reversible submonolayer growth: Monte carlo simulations*, 2008 *Phys. Rev.* B **78** 121305

[8] Aqua J-N, A Gouyé, Ronda A, Frisch T and Berbezier I, *Interrupted self-organization of SiGe pyramids*, 2013 *Phys. Rev. Lett.* **110** 096101

[9] Evans J W, Thiel P A and Bartelt M C, *Morphological evolution during epitaxial thin film growth: Formation of 2d islands and 3d mounds*, 2006 *Surf. Sci. Rep.* **61** 1

[10] Meixner M, Schöll E, Shchukin V A and Bimberg D, *Self-assembled quantum dots: Crossover from kinetically controlled to thermodynamically limited growth*, 2001 *Phys. Rev. Lett.* **87** 236101

[11] Tokar V I and Dreyssé H, *Nucleation of size calibrated three-dimensional nanodots in atomistic model of strained epitaxy: a monte carlo study*, 2013 *J. Phys.: Condens. Matter* **25** 045001

[12] Koch R, Wedler G, Schulz J J and Wassermann B, *Minute sige quantum dots on Si(001) by a kinetic 3D island mode*, 2001 *Phys. Rev. Lett.* **87** 136104

[13] Tersoff J, *Step energies and roughening of strained layers*, 1995 *Phys. Rev. Lett.* **74** 4962

[14] Tersoff J, Phang Y H, Zhang Z and Lagally M G, *Step-bunching instability of vicinal surfaces under stress*, 1995 *Phys. Rev. Lett.* **75** 2730

[15] Jesson D E, Chen K M, Pennycook S J, Thundat T and Warmack R J, *Morphological evolution of strained films by cooperative nucleation*, 1996 *Phys. Rev. Lett.* **77** 1330

[16] Li A, Liu F and Lagally M G, *Equilibrium shape of two-dimensional islands under stress*, 2000 *Phys. Rev. Lett.* **85** 1922

[17] Li A, Liu F, Petrovykh D Y, Lin J-L, Himpsel F J and Lagally M G, *Creation of quantum platelets via strain-controlled self-organization at steps*, 2000 *Phys. Rev. Lett.* **85** 5380

[18] Zandvliet H J W and van Gastel R, *Bistability in the shape transition of strained islands*, 2007 *Phys. Rev. Lett.* **99** 136103

[19] Chaparro S A, Zhang Y, Drucker J, Chandrasekhar D and Smith D J, *Evolution of Ge/Si(100) islands: Island size and temperature dependence*, 2000 *J. Appl. Phys.* **87** 2245

[20] Drucker J and Chaparro S, *Diffusional narrowing of Ge on Si(100) coherent island quantum dot size distributions*, 1997 *Appl. Phys. Lett.* **71** 614

[21] Chatterjee A and Vlachos D G, *An overview of spatial microscopic and accelerated kinetic monte carlo methods*, 2007 *Journal of Computer-Aided Materials Design* **14** 253

[22] Daruka I and Barabási A-L, *Dislocation-free island formation in heteroepitaxial growth: A study at equilibrium*, 1997 *Phys. Rev. Lett.* **79** 3708

[23] Bartelt M and Evans J, *Nucleation and growth of square islands during deposition: Sizes, coalescence, separations and correlations*, 1993 *Surf. Sci.* **298** 421

[24] Bales G S and Chrzan D C, *Dynamics of irreversible island growth during submonolayer epitaxy*, 1994 *Phys. Rev.* B **50** 6057

[25] Li M and Evans J, *Geometry-based simulation (GBS) algorithms for island nucleation and growth during sub-monolayer deposition*, 2003 *Surf. Sci.* **546** 127

[26] Mulheran P A and Blackman J A, *The origins of island size scaling in heterogeneous film growth*, 1995 *Phil. Mag. Lett.* **72** 55

[27] Mulheran P A and Blackman J A, *Capture zones and scaling in homogeneous thin-film growth*, 1996 *Phys. Rev.* B **53** 10261

[28] Kim J O, Sengupta S, Barve A V, Sharma Y D, Adhikary S, Lee S J, Noh S K, Allen M S, Allen J W, Chakrabarti S and Krishna S, *Multi-stack InAs/InGaAs sub-monolayer quantum dots infrared photodetectors*, 2013 *Appl. Phys. Lett.* **102** 011131

[29] Tokar V I and Dreyssé H, *Size distribution of atomic clusters in a model of strained submonolayer*, 2002 *Molec. Phys.* **100** 3151

[30] Tokar V I and Dreyssé H, *Lattice gas model of coherent strained epitaxy*, 2003 *Phys. Rev.* B **68** 195419

[31] Steinfort A J, Scholte P M L O, Ettema A, Tuinstra F, Nielsen M, Landemark E, Smilgies D-M, Feidenhans'l R, Falkenberg G, Seehofer L and Johnson R L, *Strain in nanoscale germanium hut clusters on Si(001) studied by x-ray diffraction*, 1996 *Phys. Rev. Lett.* **77** 2009

[32] Stepanyuk V S, Bazhanov D I, Hergert W and Kirschner J, *Strain and adatom motion on mesoscopic islands*, 2001 *Phys. Rev.* B **63** 153406

[33] Valden M, Lai X and Goodman D W, *Onset of catalytic activity of gold clusters on titania with the appearance of nonmetallic properties*, 1998 *Science* **281** 5383

[34] Landau L and Lifshitz E, 1970 *Theory of Elasticity*, (Oxford: Pergamon Press)

[35] Tokar V I and H Dreyssé, *Rigorous derivation of the rate equations for epitaxial growth*, 2013 *J. Stat. Mech.* P06001

[36] Stepanyuk V S, Bazhanov D I, Baranov A N, Hergert W, Dederichs P H and Kirschner J, *Strain relief and island shape evolution in heteroepitaxial metal growth*, 2000 *Phys. Rev.* B **62** 15398

[37] Polop C, Hansen H, Busse C and Michely T, *Relevance of nonlocal adatom-adatom interactions in homoepitaxial growth*, 2003 *Phys. Rev.* B **67** 193405

[38] Bartelt M C and Evans J W, *Scaling analysis of diffusion-mediated island growth in surface adsorption processes*, 1992 *Phys. Rev.* B **46** 12675

[39] Ross F M, Tersoff J and Tromp R M, *Coarsening of self-assembled ge quantum dots on Si(001)*, 1998 *Phys. Rev. Lett.* **80** 984

[40] Arciprete F, Fanfoni M, Patella F, Della Pia A, Balzarotti A and Placidi E, *Temperature dependence of the size distribution function of InAs quantum dots on GaAs(001)*, 2010 *Phys. Rev.* B **81** 165306

[41] Grundmann M, Stier O and Bimberg D, InAs/GaAs pyramidal quantum dots: Strain distribution, optical phonons, *and electronic structure*, 1995 *Phys. Rev.* B **52** 11969

[42] Kohmura Y, Sawada K, Fukatsu S and Ishikawa T, *Controlling the propagation of x-ray waves inside a heteroepitaxial crystal containing quantum dots using berrys phase*, 2013 *Phys. Rev. Lett.* **110** 057402